Kyushu University Global COE Program
Journal of Novel Carbon Resource Sciences, Vol. 3, pp. 11-16, Feb. 2011

Estimation of the Multi-phase Flow on the Vertical Pipe for the Methane Hydrate Recovery

Shuji Hironaka[*1], Yuki Fujisawa[*2], Saki Manabe[*2],
Gen Inoue[*3], Yosuke Matsukuma[*3], Masaki Minemoto[*3]

[*1]Graduate School of Engineering, Kyushu University
[*2]School of Engineering, Kyushu University
[*3]Faculty of Engineering, Kyushu University

(Received December 13, 2010; accepted January 11, 2011)

In this study, the experiments with two vertical pipes of different diameters were conducted to obtain the relationship between the flow rate of the gas and liquid phase. The simulation model of three-phase flow was proposed by the experimental result, which are the drag force between two-phase and the wall friction. The simulation results are good agreement in the experimental results and it was clarified that the proposed simulation model is useful to estimate the three-phase flow in the vertical pipe of the methane hydrate recovery system.

1. Introduction

Recent survey reveals there is methane gas estimated more than 100 times amount of domestic consumption in 2007 on the seabed near Japan in the form of hydrate[1]. It is methane hydrate (MH), which is stable crystal like an ice under the condition of low temperature and high pressure and formed by water molecules' trapping a methane molecule. The MH is expected as one of new energy resource[2] for Japan. The present platform designed for oil or natural gas is, however, not applicable for MH recovery because they are designed for fluid resources, not for solid. Then, several kinds of system have been studied to recover the MH such as low pressure method[3], heat injection method, inhibitor injection method, decomposition method, CO_2 hydrate replacing method[4] and gas lift method. Each of them has both of advantages and disadvantages. For example, the heat injection method has disadvantages that heat-loss of hot water would be a serious problem though it has been examined and most come into practical use at the Mackenzie, Canada[5]. In the present paper, we focused on the gas-lift method because it could have the advantage of lower running cost over the other methods[6]. It is because of self-gas-lift effect of MH. It says that the decomposition of MH might have additionally effects as same as injection of the methane gas, which is involved by high temperature seawater and lower pressure as the hydrate is raised[7, 8]. Therefore less gas injection allows to run in smaller cost. Enough knowledge is, however, not obtained for the multi-phase flow on a large scale vertical pipe, and it prevents us from constructing the actual commercial plant. Figure 1 shows the conceptual image of gas-lift system and rough principle. The up-stream flow appears on the riser pipe by injection of methane gas in the middle of riser pipe. Taking the force balance between inside and outside of vertical pipe for this system, the following equation is obtained.

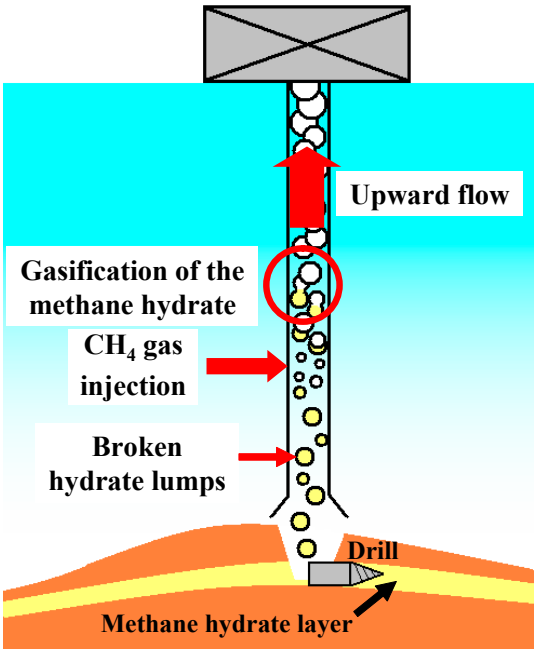

Fig. 1 Conceptual image of gas-lift system.

(Pressure at the bottom) - (Pressure at the Top) + (Pressure drop by wall friction)= (Hydrostatic pressure difference between top and bottom) (1)

Therefore,

$$(1-\varepsilon)\rho_l gH + 4f\frac{1}{2}\frac{H}{D}\rho_l U_l^2 = \gamma\rho_l gH \quad (2)$$

and we can estimate the superficial velocity of water by the eq. (3), assuming other variables is constant.

$$U_l = \sqrt{\frac{(\varepsilon+\gamma-1)gD}{2f}} \quad (3)$$

Here, γ is submerge ratio given by following equation.

$$\gamma = L_s/H \quad (4)$$

It is the ratio of the length of recovery pipe under the sea surface to its total length. However, eq. (3) will not be accurate as the amount of injected gas becomes larger because the drag force between gas and liquid phases is not negligible. This drag force is different from the system and various experiments and simulations[9] have been conducted. On the other hand, from the view to apply the gas-lift system, large number of studies on the multi-phase flow have been conducted[10]. They are, however, usually assumed that the phase transition will not occur. In the paper, we will show results of experiment with two vertical riser pipes of different diameters in the laboratory scale to measure the relationship between superficial velocity of the injection air and water. Next, the numerical simulation was conducted to the experimental system with one-dimensional multi-fluid model, and compared with experimental result. And finally, the one-dimensional simulation of the three-phase flow was carried out in the actual scale with the proper model equations, including the heat transfer between hydrate and seawater, and hydrate's decomposition.

2. Experiment

Figure 2 shows schematic of an experimental apparatus. The riser pipe (I) is made of acryl, downcomer (II) is of vinyl chloride (PVC), and both of them are connected with two acryl tanks at the top and bottom. Experiments were conducted with two kind of diameter of riser pipe: 50 *mm* and 230 *mm*, and the height were 5.5 *m* and 5.73 *m*. These apparatus have the extra pipe (III) to measure the static surface level for the submerge ratio. The air and water were used as gas and liquid phase. The orifice-like injection hole were set at 4.4 *m* deep for 50 *mm* riser pipe, and 4.63 *m* for 230 *mm* from top of riser pipe. Air is injected by the (IV) compressor through the (V) dryer and it makes up-stream two-phase flow on the riser pipe. Flow rate of air and water were recorded by mass flow meter (VI) and electromagnetic flow meter (VII) respectively.

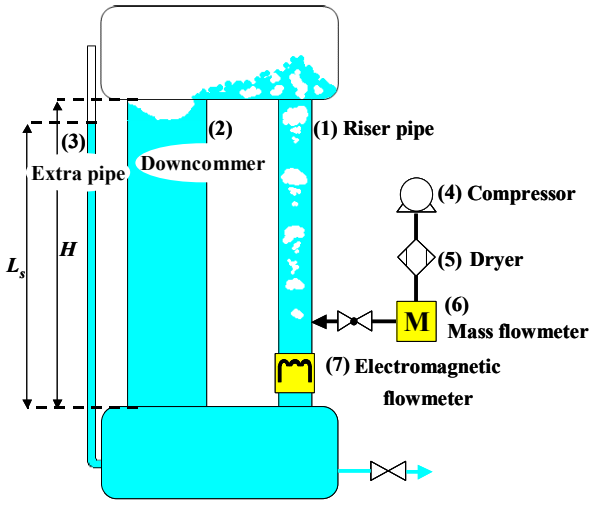

Fig. 2 Schematic of experimental apparatus.

The volume flow rate of water and that of injected gas were measured to obtain the superficial velocity.

According to eq. (3), water superficial velocity will depend on the submerge ratio. Therefore, we paid attention to keep it almost same in recording the superficial velocity by adjusting the amount of water on the apparatus.

Figures 3 and 4 show the dependence of the water superficial velocity on the gas superficial velocity when the submerge ratio was changed from 0.95 to 0.99 at 0.01 intervals for 50 *mm* and 230 *mm* diameter pipe respectively. They also show the water superficial velocity is influenced by the submerge ratio, because of the larger hydrostatic pressure.

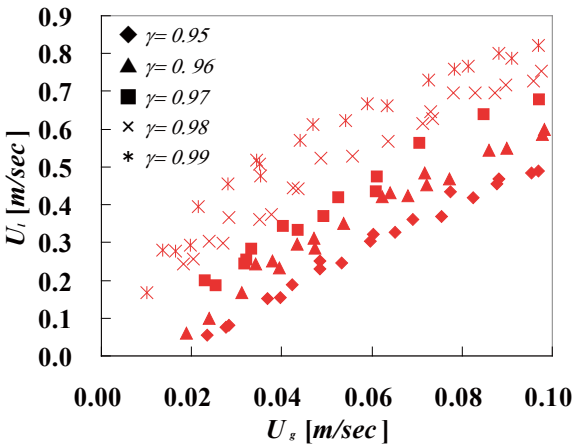

Fig. 3 U_l's dependence on U_g (50 *mm* Diameter).

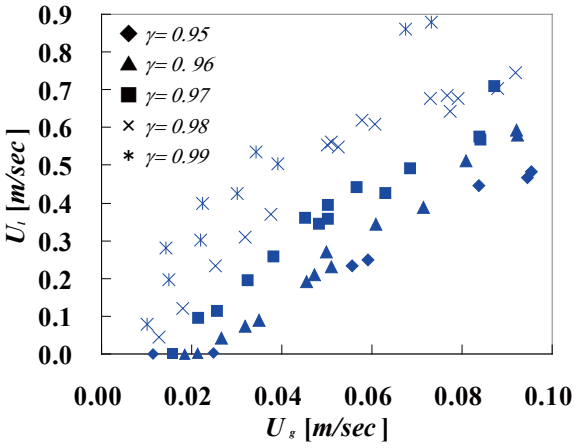

Fig. 4 U_l's dependence on U_g (230 *mm* Diameter).

3. Numerical simulation

3.1 Assumptions

Basic equations for numerical simulation were derived based on the multi-fluid model, which is to solve the pressure, volumetric fractions, and velocity of each

phase. The following assumptions were set to conduct the calculation:

I) The multi-phase flow is assumed as the one-dimensional flow on the riser pipe.
II) Riser pipe does not have any flexures, thus its cross sectional area is uniform.
III) The bubble form is spherical in the bubble flow region.
IV) The contracted coefficient at the bottom of the r iser pipe was 1.0.
V) All phases exist under the same pressure.
VI) Form of solid phase is spherical.
VII) Only gas density changes depending on the pressure and temperature, and other phase densities are constant.
VIII) For the temperature of each phase, the gas and liquid's is equal, and the solid temperature is equilibrium temperature of the methane hydrate under the surrounding pressure. Its distribution through the solid sphere is uniform.
IX) The heat transfer is only considered for the liquid phase.
X) The decomposed hydrate or ice is NOT reformed again.

3.2 Equations

Concrete equations are given by following eqs. (5) ~ (8).

$$\frac{\partial}{\partial t}\left(\alpha_k \rho_k\right)+\frac{\partial}{\partial x}\left(\alpha_k \rho_k v_k\right)=K \tag{5}$$

$$\frac{\partial}{\partial t}\left(\alpha_k \rho_k v_k\right)+\frac{\partial}{\partial x}\left(\alpha_k \rho_k v_k^2\right)=-\alpha_k \frac{\partial p}{\partial x}-\left(fric,k\right)v_k - \sum_{k' \neq k}\left(inter\right)_{kk'}\left(v_k - v_{k'}\right)-\rho_k \alpha_k g - K v_k \tag{6}$$

$$\sum \alpha_k = 1 \tag{7}$$

$$\rho_l \alpha_l C_p\left(\frac{\partial T_l}{\partial t}+v_l \frac{\partial T_l}{\partial t}\right)=Q_{wall}+Q_{ls} \tag{8}$$

Eq. (5) is the equation of mass conservation, eq. (6) represents the momentum conservation, eq. (7) is the definition of volumetric fraction, and eq. (8) shows the heat conservation on the liquid phase. K denotes the amount of transition of the each phase, and they are given by following equations respectively.

$$S=-\frac{6\alpha_s}{d_s}\cdot\frac{h_{ls}\left(T_l-T_s\right)}{H_{decomp}\theta_p} \tag{9}$$

$$L=-\left(1-\sigma_{CH_4}\right)\theta_p S \tag{10}$$

$$G=-\sigma_{CH_4}\theta_p S \tag{11}$$

3. 3 Constitutive Equations

Several terms appearing basic equations are semi-experimentally given by the following constitutive equations. For wall friction term, it is given by following eq. (12).

$$\left(fric,k\right)=\frac{2mf_m}{D}w_k \rho_k \alpha_k \left|v_k\right| \tag{12}$$

Here,

$$m=\begin{cases}4.8+0.4\ln\alpha_g & \alpha_g < 0.2\\ 4.2 & \alpha_g \geq 0.2\end{cases} \tag{13}$$

$$f_m=\begin{cases}16/Re_m & Re_m < 2300\\ 0.0791/Re_m^{0.25} & Re_m \geq 2300\end{cases} \tag{14}$$

$$w_g=\begin{cases}0 & \alpha_g \leq 0.9\\ \left(10\alpha_g-9\right)^2\left(21\alpha_g-20\right) & \alpha_g \geq 0.9\end{cases} \tag{15}$$

$$w_l = 1 \tag{16}$$

$$w_s = 0 \tag{17}$$

Eq. (14) is the Blasius' equation, and it is only applicable to the single phase. Therefore, it is required to define the Reynolds number to the mixture fluid to apply the gas-liquid two-phase flow.

$$Re_m=\frac{\left|\alpha_g \rho_g v_g+\alpha_l \rho_l v_l\right| D}{\left(\alpha_g \mu_g+\alpha_l \mu_l\right)} \tag{18}$$

The drag force between gas and liquid phase is defined by eq. (19).

$$\left(inter\right)_{lg}=\frac{1}{8}C_{d,l}a\rho_l\left|v_g-v_l\right| \tag{19}$$

$$C_{d,l}=\begin{cases}0.54\alpha_g^{-0.48} & 0<\alpha_g \leq 0.75\\ \frac{8}{3}\left(\frac{1-\alpha_g}{1-\alpha_{gs}}\right)^2 & 0.75<\alpha_g \leq 1\end{cases} \tag{20}$$

$$a=\begin{cases}\frac{6\alpha_g\left(0.3+0.2\alpha_g\right)}{d_g} & 0<\alpha_g \leq 0.25\\ \frac{4.5}{D}\cdot\frac{\alpha_g-\alpha_{gs}}{1-\alpha_{gs}}+\frac{6\alpha_{gs}}{d_g}\cdot\frac{1-\alpha_g}{1-\alpha_{gs}} & 0.25<\alpha_g \leq 1\end{cases} \tag{21}$$

Moreover, the averaged gas volume fraction for the slug flow and the bubble diameter is given by following equations.

$$\alpha_{gs} = \begin{cases} \alpha_g & \left(0 \le \alpha_g < 0.25\right) \\ 0.3929 - 0.5714\alpha_g & \left(0.25 \le \alpha_g < 0.715\right) \\ 0.05 & \left(0.715 \le \alpha_g < 1\right) \end{cases} \quad (22)$$

$$d_g = 0.95 D U_g^{0.2} \quad (23)$$

Similarly, the drag force between liquid and solid phase is also defined by eq. (24).

$$\left(inter\right)_{ls} = \frac{1}{8} C_{d,s} \left(\frac{6\alpha_s}{d_s}\right) \rho_l \left|v_l - v_s\right| \quad (24)$$

And the drag force coefficient between liquid and solid, and the solid diameter in eq. (24) are given by following eq. (25) and (26).

$$C_{d,s} = \begin{cases} 24/Re_p & Re_p \le 2 \\ 10/Re_p^{0.5} & 2 < Re_p \le 500 \\ 0.44 & 500 < Re_p \end{cases} \quad (25)$$

$$d_s = d_{s0} \left(\frac{\alpha_s}{\alpha_{s0}}\right)^{1/3} \quad (26)$$

Here, $Re_p = \dfrac{\rho_l \left|v_s - v_l\right| d_s}{\mu_l}$.

The density of gas phase is given by the equation of the state for the ideal gas because of the compressibility.

$$\rho_g = \frac{M_{CH_4} p}{R T_l} \quad (27)$$

Additionally, the temperature of the solid phase is same to the equilibrium temperature of the methane hydrate as a function of the pressure.

$$T_s = \frac{8533.8}{38.98 - \ln\left[p/\left(1.013\times10^5 \times 9.869\times10^{-3}\right)\right]} \quad (28)$$

The following equations represent the term of the heat exchange between the liquid and wall or solid phase in the eq. (8) respectively.

$$Q_{wall} = -\frac{4U\left(T_l - T_{sur}\right)}{D} \quad (29)$$

$$Q_{ls} = -\left\{\left(\frac{6\alpha_s}{d_s}\right) h_{ls}\left(T_l - T_s\right) + \frac{T_l L}{\rho_l \alpha_l}\right\} \quad (30)$$

4. Result and discussion

The simulation was compared with the experiment showed in the section 2 to evaluate the simulation model. Figures 5 and 6 show the comparison between calculation and experiment with γ changed for two different diameters, 50 *mm* and 230 *mm*. Since the experiment was conducted in the gas-liquid two-pahse system, the solid phase is neglected. The experimental results are dotted and simulations are lined. Simulation results fairly agreed with the exepriment in the case of diameter D = 50 *mm*. Although the calculation results underestimate liquid superficial velocity in the case of D = 230 *mm* especially at the high gas velocity region, it shows the similar qualitative tendency to the experiment. In order to consider of the reason why the simulation underestimated the liquid superficial velocity, the ratio between the interface drag force and wall friction is taken with eq. (12) and (19).

$$\frac{\left(fric,l\right)}{\left(inter\right)} = \frac{16 f_m \alpha_l}{D C_{d,l} a \left(1 - v_g/v_l\right)^2} \quad (31)$$

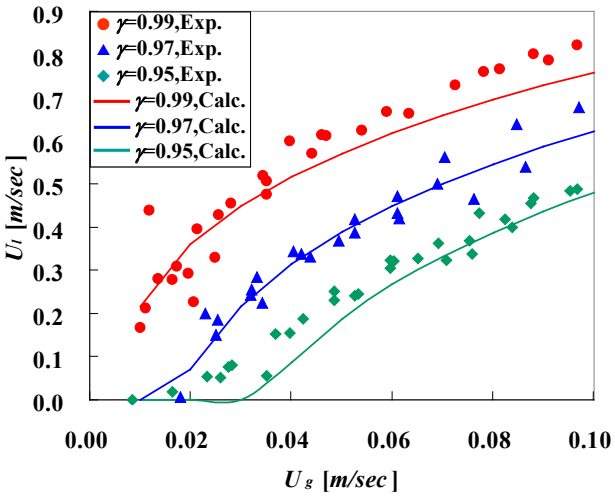

Fig. 5 U_l's dependence on U_g (50 *mm* Diameter).

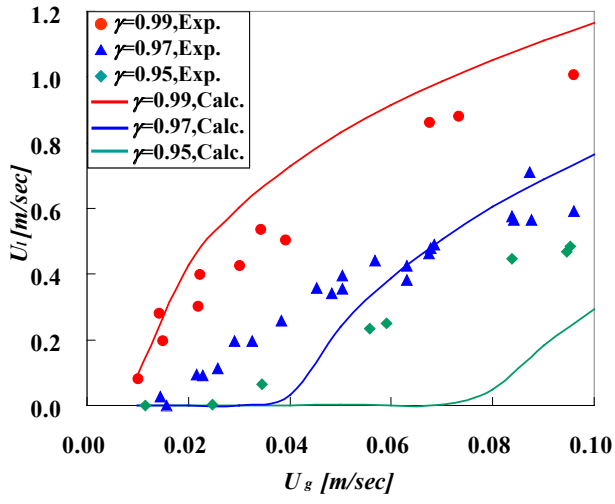

Fig. 6 U_l's dependence on U_g (230 *mm* Diameter).

In eq. (31), the ratio between gas and liquid velocity, interfacial area density, and drag force coefficient become more effective as the submerge ratio is smaller, and the amount of the injection air is larger despite that wall friction coefficient and liquid volume fraction are almost constant. Therefore, eq. (31) shows that the inter-phase drag force is more dominant under the condition of the smaller submerge ratio, larger air injection, and larger pipe diameter. In conclusion, the present calculation model is necessary to be improved if it is necessary to calculate under the condition of the small submerge ratio.

Since it is obvious that the effect of the inter-phase drag force is negligible to the present calculation model under the condition of the larger submerge ratio around 0.99, the estimation of the actual system is conducted with the submerge ratio set in 1.00. The effect of hydrate decomposition was considered in this simulation. The calculation condition is shown in Table 1.

Table 1 Calculation condition

Item	Value	Unit
Diameter of riser pipe	0.47	[*m*]
Length	500.0	[*m*]
Injection depth	250.0	[*m*]
Heat conductivity of the pipe wall	15.0	[*W/(m·K)*]
Thickness of the pipe	0.019	[*m*]
Gas superficial velocity	0.5	[*Nm/sec*]
Submerge ratio	1.00	[-]
Temperature of liquid phase at the surface	277.0	[*K*]
Density of liquid phase	1024.0	[kg/m^3]
Density of solid phase	2100.0	[kg/m^3]
Diameter of solid at the inlet	0.01, 0.05	[*m*]
Volume fraction of the hydrate at the inlet	5.0	[*vol.%*]
Decomposition enthalpy of hydrate	450, 000	[*J/kg*]
Porosity	0.3	[m^3-*pore*/m^3-*sol.*]
Saturation ratio of the CH_4	0.05	[m^3-CH_4/m^3-*pore*]

Figures 7, 8 and 9 represent the distribution of the velocity, volume fraction, decomposition rate and diameter of the solid phase respectively. The x axis is directed to the sea surface with set the origin at the bottom of the riser pipe (seabed) in all these 3 figures. In Figure 7, the velocity of the gas phase appears at the deeper region because of the decomposition of the hydrate. Since the gas hydrate completely decomposes before reaching at the sea surface, the solid velocity disappears at the middle point. Moreover, this figure also shows the fundamental qualitative tendency that the small solid is easier to recover than the larger solid. Figure 8 is the distribution of the volume fractions of the each phase in two cases for the solid diameter at the inlet. The gas phase suddenly expands especially around the sea surface because the pressure decreases. As a result, its volume fraction becomes large, and the liquid's fraction is small. As we saw in the previous figure, the gas expansion also involves the increase of the velocity of the each phase to satisfy the mass balance on the arbitrary control volume. Finally, Figure. 9 shows the decomposition ratio of the solid phase on the left hand and the solid diameter on the right. The decomposition rate is large in the case to recover the solid of 0.01 *m* diameter compared with the result of the 0.05 *m* diameter. It corresponds to the large mass flow rate of the solid phase in the case of small diameter as it was previously denoted. Additionally, it shows the large solid decomposes more slowly than the case of the small diameter. Results in both cases suggest that the gas-lift system will be economical to run because the complete decomposition of the methane hydrate allows to cut down the amount of the injection CH_4 gas.

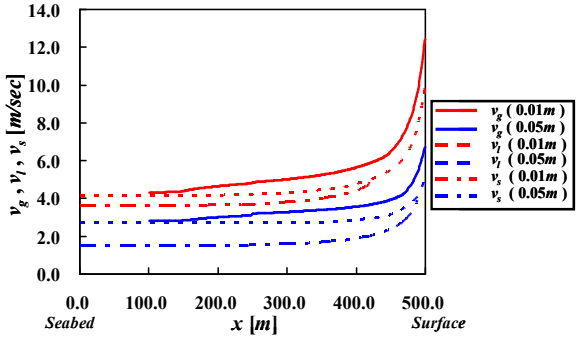

Fig. 7 Distribution of the velocity of the each phase.

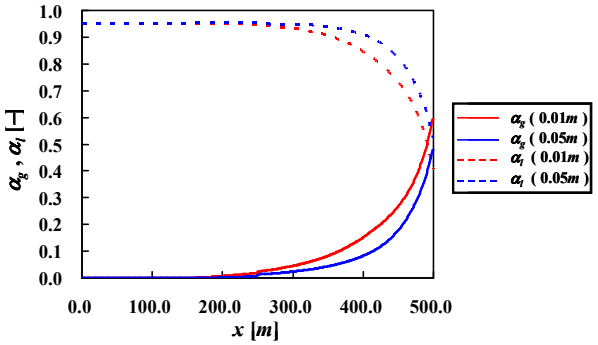

Fig. 8 Distribution of the volume fraction of the gas and liquid phase.

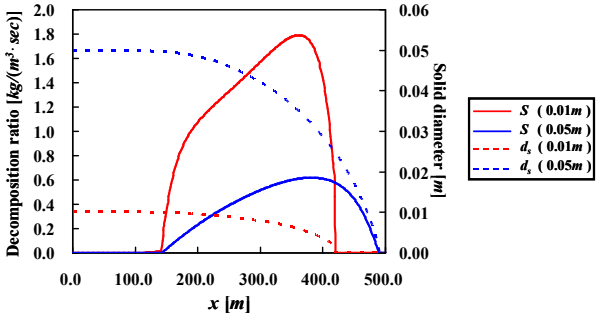

Fig. 9 Distribution of the decomposition ratio and solid diameter of the solid phase.

5. Conclusion

The gas-lift experiment is conducted in the laboratory scale, and the simulation model is proposed to apply the one-dimensional two-fluid model. The numerical simulation fairly agreed with the experiment for the relationship between the gas and liquid flow rate in the large submerge ratio. However, it is not able to estimate the liquid superficial velocity under the small submerge ratio, and it is because of the inter-phase drag force model. Then, the multi-phase flow on the actual system is estimated with the proposed model, and the decomposition of the hydrate considered. As a simulation result, the methane hydrate will completely decompose and it showed the gas-lift system can be an economical running system to recover the methane hydrate.

References

1) M. Sato, *J. the Japan Institute of Energy*, **80**, 635 (2002).
2) S. Y. Lee, G.D. Holder, *Methane hydrates potential as future energy sources fuel processing technology*, **71**, 181 (2001).
3) Y. Masuda, *Aquabiology*, **23**, 478 (2001).
4) I. Aya, K. Yamane, T. Kojima, S. Namie, *The high-pressure science and technology for the oceanic CO_2 isolation and CO_2 hydrate*, **12- 1**, 40 (2002).
5) R. Hamaguchi *et al.*, *Kagaku Kogaku Ronbunshuu*, **31**(1), 68 (2005).
6) R. Gregor, *Geochimica et Cosmochimica Acta.*, **64**, 285 (2004).
7) S. K. Kelkar, *Hydrate dissociation rates in pipelines Fluid Phase Equilibria*, 371 (1998).
8) M.Ishii,K.Mishima,I.Kataoka,G.Kocamustafaogullari, *Proc 9th U.S. National Congress of Applied Mechanics*, 73 (1982).
9) S. Michio, N. Kawahara, T. Kimura, J. Nakao, *Kikai Gakkai Ronbunshuu(B)* **74-742**, 1263 (2008).
10) T. Yoshinaga, Y. Sato, *Int. J. Multihphase Flow*, **22**(2), 223 (1996).

Nomenclature

Letters

a	: Interfacial area density between liquid and gas phase	[$1/m$]
C_p	: Heat capacity per unit mass at constant pressure	[$J/(K \cdot kg)$]
$C_{d,l}$	: Drag force coefficient between liquid and gas phase	[-]
$C_{d,s}$	: Drag force coefficient between liquid and solid phase	[-]
D	: Pipe diameter	[m]
d_g	: Bubble diameter	[m]
d_s	: Solid diameter	[m]
d_{s0}	: Solid diameter at the inlet	[m]
f, f_m	: Wall friction coefficient	[-]
g	: Gravitational acceleration	[m/sec^2]
$(fric,k)$	: The wall friction of the each phase	[$kg/m^3 \cdot sec$]
H	: Pipe length	[m]
H_{decomp}	: Decomposition enthalpy of the methane hydrate	[J/kg]
h_{ls}	: Heat transfer coefficient between liquid and solid	[$W/(m \cdot K)$]
$(inter)$	: Inter-phase drag force	[$kg/m^3 \cdot sec$]
K	: Amount of the decomposed/generated mass for the each phase (K= G, L, S)	[$kg/m^3 \cdot sec$]
L_s	: Static surface level	[m]
M_{CH_4}	: Molar weight of the methane	[kg/mol]
m	: Modification factor of the wall friction	[-]
p	: Pressure	[Pa]
Q_{ls}	: Heat exchanged between liquid and solid	[W/m^s]
Q_{wall}	: Heat exchanged between liquid and wall	[W/m^s]
R	: Gas constant	[$J/(K \cdot mol)$]
T	: Temperature	[K]
U	: Overall heat transfer coefficient of the riser pipe	[$W/(m \cdot K)$]
U_k	: Superficial velocity	[m/sec]
v	: Velocity	[m/sec]
w	: Distribution factor of the wall friction	[$kg/m^3 \cdot sec$]
α	: Volume fraction	[-]
α_{gs}	: Averaged gas volume fraction for the slug flow	[-]
α_{s0}	: Solid volume fraction at the inlet	[-]
γ	: Submerge ratio	[-]
ε	: Gas volume fraction averaged on the whole riser pipe	[-]
θ_p	: Porosity	[-]
μ	: Viscosity	[$Pa \cdot sec$]
ρ	: Density	[kg/m^3]
σ_{CH_4}	: Saturation ratio of the methane to the porous part	[-]

Subscriptions

k	: Focused phase (k= g, l, s)
k'	: The other phase
g, l, s	: Gas phase, liquid phase, and solid phase